

## NONLINEAR FINITE ELEMENT MODELING OF PRESTRESSED LEAD EXTRUSION DAMPERS

F. Çalım<sup>1\*</sup>, A. Güllü<sup>2</sup>, C. Soydan<sup>3</sup>, and E. Yüksel<sup>1</sup>

<sup>1</sup> Faculty of Civil Engineering, Istanbul Technical University  
Maslak, 34485 Sariyer, Istanbul, Türkiye  
[calimf@itu.edu.tr](mailto:calimf@itu.edu.tr), [yukselerc@itu.edu.tr](mailto:yukselerc@itu.edu.tr)

<sup>2</sup> Ingram School of Engineering, Texas State University  
San Marcos, TX 78666, USA  
[ahmetgullu@txstate.edu](mailto:ahmetgullu@txstate.edu)

<sup>3</sup> Department of Civil Engineering, Tekirdag Namik Kemal University  
59030 Suleymanpasa, Tekirdag, Türkiye  
[csoydan@nku.edu.tr](mailto:csoydan@nku.edu.tr)

---

### Abstract

*In the earthquake-resistant design of the structures, supplemental energy dissipative devices have increasingly been utilized for structural response control. The lead extrusion damper (LED) is one of the prominent versions of metallic dampers, as it dissipates high amounts of seismic energy by the extrusion of lead through the displacement of a bulged shaft. Its geometric properties, i.e., length and diameter of the tube, shaft, bulge, and lead, should be designed based on the target performance level of the host structural system. Thus, determining the LED's force-displacement relationship and seismic energy dissipation characteristics becomes essential for a proper design. In this study, the developed three-dimensional finite element modeling (FEM) strategy for the LED is examined through some literature experiments. The comprehensive three-dimensional model was utilized with the exact material characteristics determined through the coupon tests to increase the accuracy of predicting the LED's behavior. The numerical models were verified using the experimental results of the LEDs with different geometries adapted from the literature. The low relative differences between the numerically and experimentally obtained damper forces, i.e., 4.3% mean error, exhibited that the developed modeling strategy can accurately simulate the LED's hysteretic behavior. The consistency of the modeling strategy with different devices' behavior proved the versatility of the developed FEM. In addition, the effects of the different geometric properties on the LED's cyclic behavior were discussed numerically.*

**Keywords:** Finite Element Analysis, High Force-to-Volume, Lead Extrusion Damper, Passive Energy Dissipater, Seismic Energy Dissipation.

## 1 INTRODUCTION

The seismic energy imparted into the structures converts into kinetic energy ( $E_k$ ), damping energy ( $E_d$ ), and strain energy ( $E_s$ ). The  $E_s$  term comprises recoverable elastic and irrecoverable inelastic (hysteretic) energy terms. This energy must be dissipated to prevent life and financial losses during seismic excitations. Based on the conventional earthquake-resistant design practice, it is dissipated through structural members' internal damping and hysteretic behavior. On the other hand, the modern earthquake-resistant design practice promotes using supplementary energy dissipative devices as fuse elements. The purpose is to protect new structures and retrofit the existing ones against nonstructural and structural damage due to strong ground motions [1-4].

A lead extrusion damper (LED) is a metallic damper utilizing a passive control system, and it employs the hysteretic energy dissipation characteristics of lead by an extrusion process. For this process, either a constricted tube or a bulged shaft is utilized [5-6]. The damper has three main components: lead, steel shaft, and steel cylinder.

LED has been a preferable energy dissipative device in recent years for several advantages. Since lead is a very soft metal with a high plastic deformation capacity, it can be employed in energy dissipation even under small displacements. It returns to its original state through recrystallization [7-8]. This phenomenon provides the recentering ability to the device, which results in being free of additional maintenance costs after an earthquake. Also, LED is unaffected by aging effects and environmental factors, and its load-deformation curves remain stable [9]. In addition, the low-cycle fatigue effect is insignificant for the device since lead is the only part going under plastic deformations [10].

Other than the geometric properties of the device, the amount of dissipated energy mainly depends on if the lead inside the tube is prestressed. The prestressing procedure results in less void formation inside the lead, consequently improving the damping properties. Thus, LEDs can be produced as high force-to-volume (HF2V) devices by achieving high damper forces even with smaller device dimensions when the lead is prestressed [11].

Several research groups have produced LEDs with different design approaches and geometric properties [12-17]. Later, the efficiency of LEDs was experimentally and analytically proven for the seismic response control of structures such as beam-to-column connections [18], frames [19], damage-free steel connections [20], interconnected structures [21], precast buildings [22].

This study numerically investigated the effects of the different geometric properties on the energy dissipation characteristics of LEDs. For this purpose, some literature examples, which have experimentally been tested, were adapted for finite element modeling.

## 2 LEAD EXTRUSION DAMPERS

The geometric properties of the LEDs modeled in this study were adapted from the literature study of Vishnupriya et al. [23]. The section view for the devices is illustrated in Figure 1. The LEDs have a bulged shaft, which extrudes the lead from the gap between the bulge and the tube.

The geometric properties, i.e., the diameter of the cylinder ( $D_{cyl}$ ), the diameter of the bulge ( $D_{blg}$ ), the diameter of the shaft ( $D_{shaft}$ ), the length of the cylinder ( $L_{cyl}$ ), the length of the bulge ( $L_{blg}$ ), and the length of the bulge's flat section ( $L_{blg\_flat}$ ), are shown in Table 1 for the modeled LEDs. The dampers have a constant shaft diameter of 30 mm, whereas all other geometric properties are varying parameters.

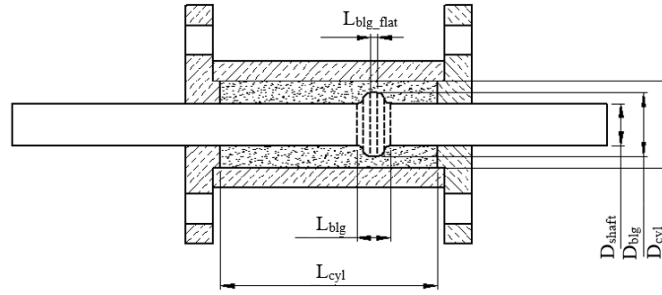


Figure 1: Section view of the modeled LEDs.

Table 1: Geometric properties of the modeled LEDs [23].

LED #	D <sub>cyl</sub> (mm)	D <sub>blg</sub> (mm)	D <sub>shaft</sub> (mm)	L <sub>cyl</sub> (mm)	L <sub>blg</sub> (mm)	L <sub>blg_flat</sub> (mm)
1	89	50	30	110	30	5
2	89	58	30	110	30	5
3	66	40	30	130	30	6
4	66	50	30	130	30	5
5	54	35	30	160	20	3
6	54	38	30	160	20	3

### 3 FINITE ELEMENT MODELING

The three-dimensional modeling strategy adapted by Çalım et al. [24] was utilized in developing the finite element models in Abaqus FEA software [25]. Each component of the LEDs was modeled as three-dimensional deformable parts, and solid, homogenous sections were assigned to each part.

To properly simulate the nonlinear material property of lead, true stress-strain data computed through standard tension tests of Çalım et al. [24] was used. It also accounts for the degrading part of the material's stress-strain curve, unlike the material model used by Vishnupriya et al. [23], Figure 2. Young's modulus and Poisson's ratio were defined as 9 MPa and 0.44, respectively, for the elastic behavior of the lead. On the other hand, a combined isotropic/kinematic hardening model with the "Half Cycle" option was employed to consider ratcheting and cyclic hardening effects in modeling the inelastic behavior.

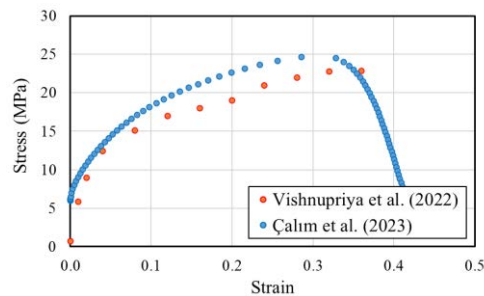


Figure 2: Plastic material data for lead.

The movement of the cylinder was restricted by assigning an "encastre" (fixed) type boundary condition to both ends. Standard surface-to-surface contact interaction was defined between the steel and lead surfaces with a friction coefficient of 0.25. The effects of nonlinearity caused by both material and geometry were considered in the finite element models. In addition, C3D8R-type elements (8-node linear brick, reduced integration with an

hourglass control element) were adapted for the three-dimensional meshing of the finite element models.

Two diverse models were generated for each LED. In the first model, a ramp-type amplitude was applied to the shaft through a displacement/rotation-type boundary condition. This model was used to validate the finite element models since the LEDs were tested under monotonic loading in the experimental study. In the second model, a sinusoidal displacement procedure with an amplitude of 5 mm was applied to the shaft. This model was used for the numerical investigation of the LEDs' cyclic behavior.

## 4 RESULTS AND DISCUSSION

### 4.1 Experimental validation

First, the finite element models were validated through the experimental data. The LEDs studied in this paper have experimentally been tested under a monotonically increasing displacement pattern [23]. Thus, the force-displacement curves of devices under a ramp-type loading were compared with the experimental ones, as illustrated in Figure 3.

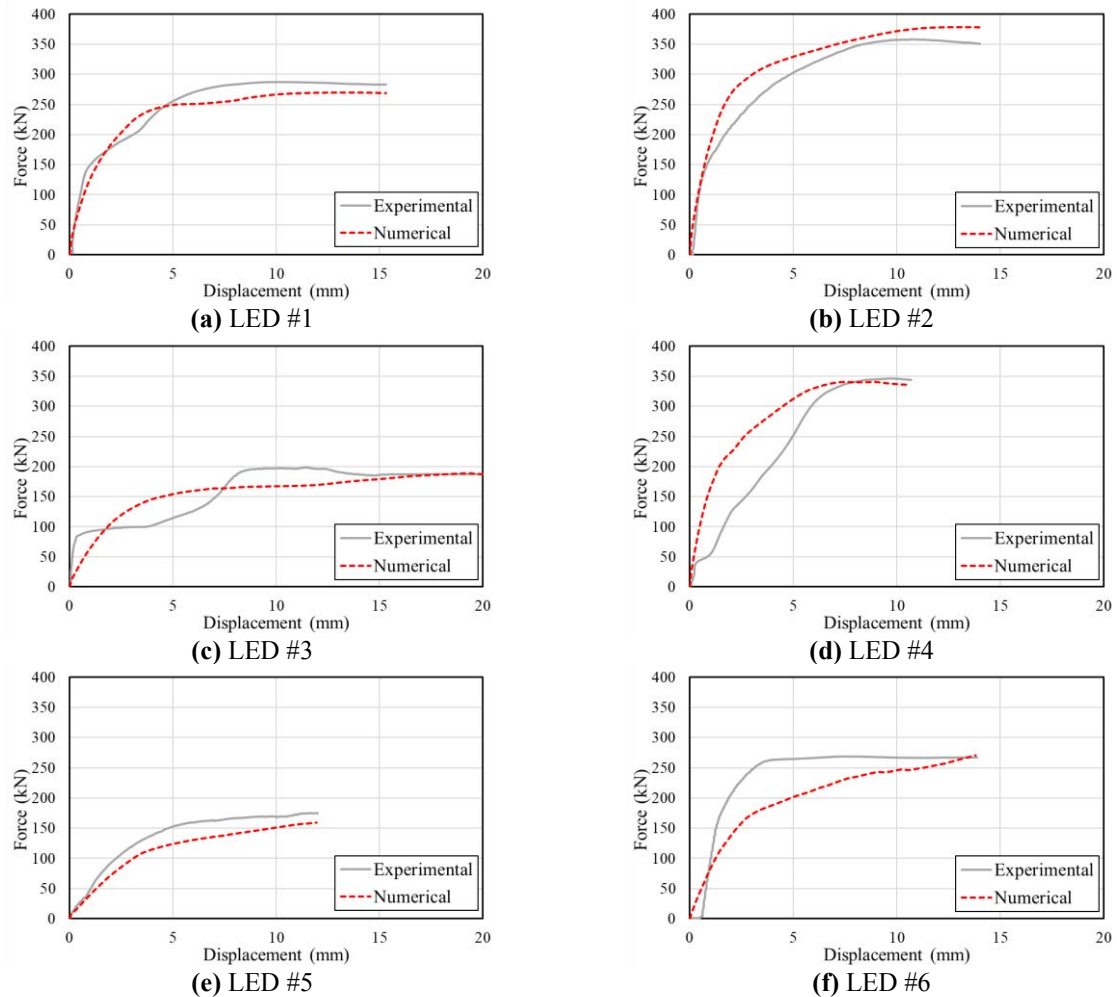


Figure 3: Experimental validation of the finite element models.

Experimentally and numerically computed damper forces are presented in Table 2. The relative differences between them are also displayed in the table, where “+” represents an overestimation and “-” represents an underestimation in the damper force predictions. The

low relative differences in the damper force predictions proved the accuracy of the adapted finite element modeling strategy. While the maximum relative difference in the damper force prediction for six LEDs was 5.9% (LED #1 and #5), the absolute average value was 4.3%.

Table 2: Damper force comparisons.

LED #	Experimental Damper Force (kN)	Numerical Damper Force (kN)	Relative Difference (%)
1	287	270	-5.9
2	358	378	+5.6
3	199	188	-5.5
4	346	340	-1.7
5	170	160	-5.9
6	268	271	+1.1

## 4.2 Analysis of the numerical results

After validating the finite element models using the experimental data, a sinusoidal displacement pattern with an amplitude of 5 mm was applied to the LEDs to compare their cyclic behavior. The achieved hysteresis curves are presented in Figure 4 for each damper.

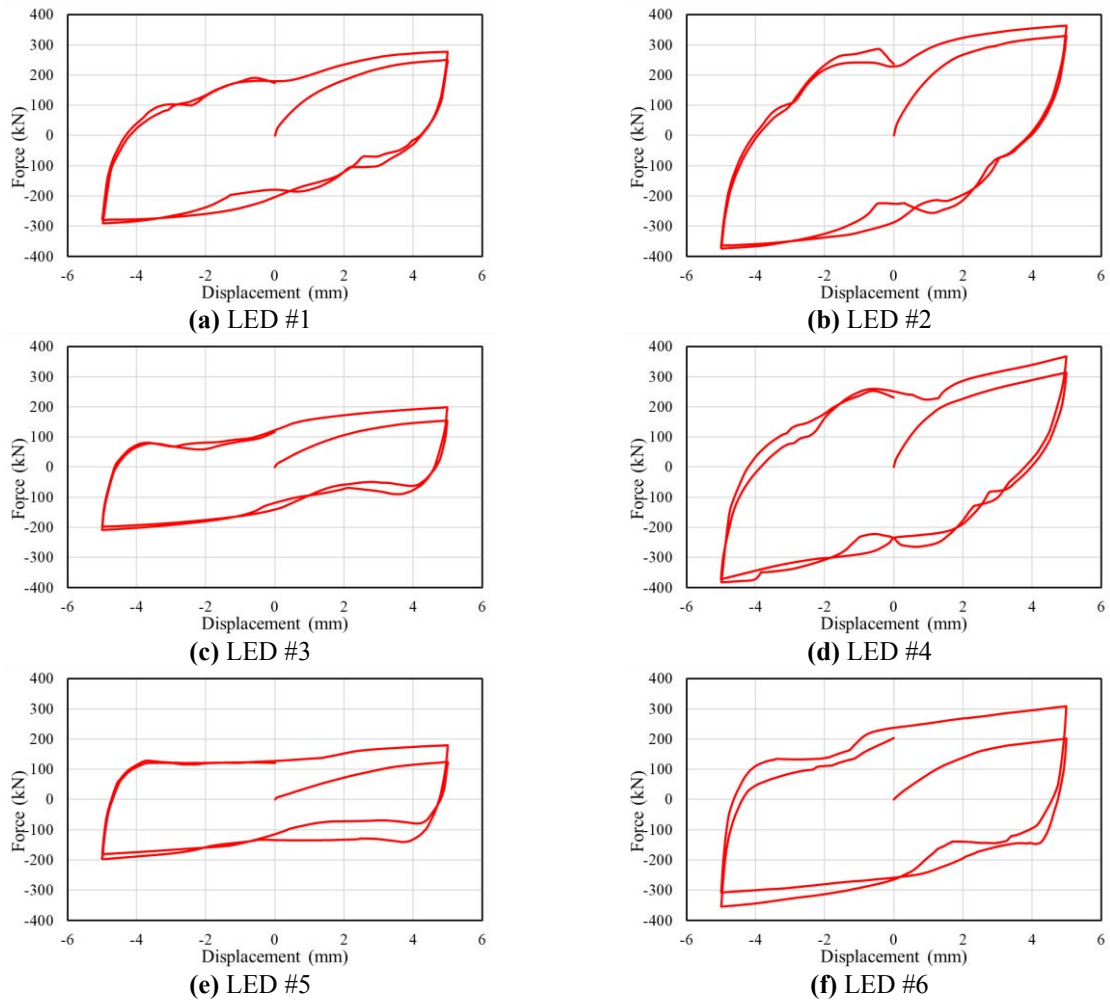


Figure 4: Hysteresis curves of the LEDs.

A loop discretization method was applied to the hysteresis curves to calculate the amounts of dissipated energy in each cycle. As a result, they were computed as 3307.8, 4317.5, 2446.3, 4042.8, 2723.7, and 4226.2 kN·mm, respectively, for each damper.

The relationships between the geometric properties and behavior of the dampers were also investigated. For this purpose, the damper force ( $F_d$ ) and the amount of dissipated energy ( $E_D$ ) were correlated with the bulge diameter ( $D_{blg}$ ), the cross-sectional area of lead ( $A_{lead}$ ), and the ratio of the cross-sectional area of the bulge ( $A_{blg}$ ) to  $A_{lead}$ , as illustrated in Figure 5. Here, each blue point represents the behavior of a single damper. In addition, the linear trendlines that best fit the data points and their equation are displayed in the figures.

The best fit was achieved for the  $F_d - D_{blg}$  (Figure 5a) and  $F_d - A_{blg}/A_{lead}$  (Figure 5c) relationships. The R-squared value, which measures the trendline reliability, was around 0.8 for both cases. It can be concluded that the damper force is mainly dependent on the bulge geometry, and it can reliably be estimated through  $D_{blg}$  or the ratio of  $A_{blg}$  to  $A_{lead}$ .

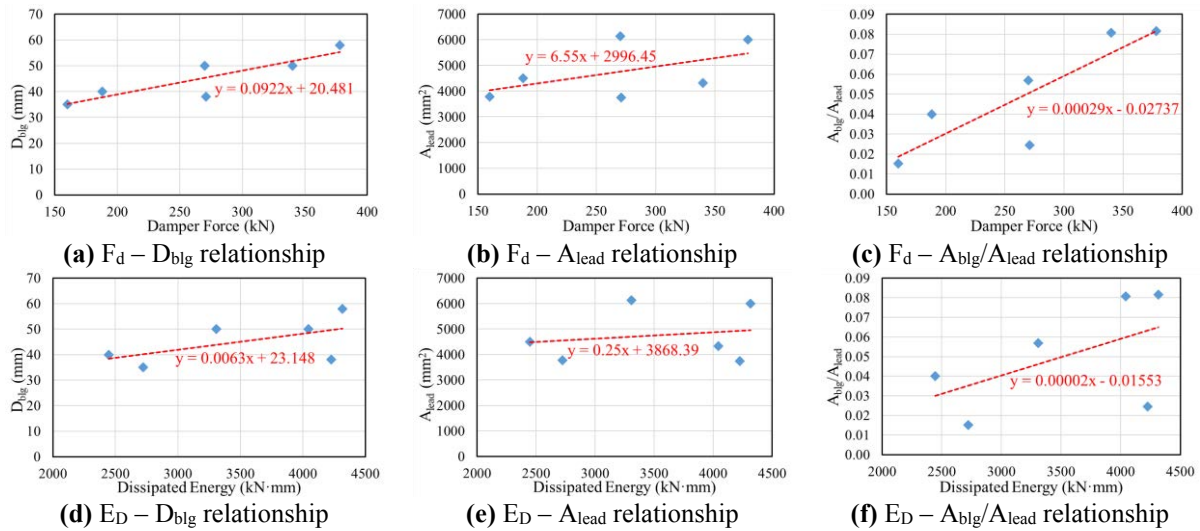


Figure 5: The relationships between the geometric properties and behavior of the dampers.

## 5 CONCLUSIONS

The nonlinear finite element models of six lead extrusion dampers (LEDs) with varying geometric properties were generated by adapting a three-dimensional modeling strategy. After the models were validated through the experimental data in the literature, cyclic analyses were conducted. As a result, the following conclusions were obtained:

- The adapted finite element modeling strategy yielded accurate results in the damper force predictions. The relative differences between the experimental and numerical damper forces ranged between 1.1% and 5.9%, with an average of 4.3%.
- The hysteresis curves were numerically obtained under a sinusoidal displacement pattern with an amplitude of 5 mm. Very stable and almost rectangular curves were achieved for each damper. For the studied geometries, the energy dissipation in each cycle was computed in the range of 2446.3 to 4317.5 kN·mm.
- The effect of different geometric properties on the damper force and energy dissipation capacities was investigated. The damper force was observed to primarily rely on the bulge's shape. It can be most effectively approximated by using the bulge diameter or the bulge-to-lead area ratio.

## ACKNOWLEDGMENTS

The study was supported by the Scientific and Technological Research Council of Türkiye (TÜBİTAK) research project 121M719. All the support is acknowledged. Additionally, the authors sincerely thank Dr. Vishnupriya and her co-authors for sharing their experimental data.

## REFERENCES

- [1] R.D. Hanson, I.D. Aiken, D.K. Nims, P.J. Richter, R.E. Batchman, State of the art and state of the practice in seismic engineering dissipation. *Proceedings of ATC-17-1 Seminar on Seismic Isolation, Passive Energy Dissipation and Active Control, Advanced Technology Council*, San Francisco, California, 1993.
- [2] I.D. Aiken, Passive energy dissipation-hardware and applications. *Proceedings of the Los Angeles County and SEAOSC Symposium on Passive Energy Dissipation Systems for New and Existing Buildings*, Los Angeles, 1996.
- [3] A.H. Barbat, L.M. Bozzo, Seismic analysis of base isolated buildings. *Archives of Computational Methods in Engineering*, **4(2)**, 153–192, 1997. <https://doi.org/10.1007/bf03020128>
- [4] T.T. Soong, B.F. Spencer, Supplemental energy dissipation: State-of-the-art and state-of-the-practice. *Engineering Structures*, **24(3)**, 243–259, 2002. [https://doi.org/10.1016/s0141-0296\(01\)00092-x](https://doi.org/10.1016/s0141-0296(01)00092-x)
- [5] W.H. Robinson, L.R. Greenbank, Properties of an extrusion energy absorber. *Bulletin of the New Zealand Society for Earthquake Engineering*, **8(3)**, 187–191, 1975. <https://doi.org/10.5459/bnzsee.8.3.187-191>
- [6] W.H. Robinson, L.R. Greenbank, An extrusion energy absorber suitable for the protection of structures during an earthquake. *Earthquake Engineering and Structural Dynamics*, **4(3)**, 251–259, 1976. <https://doi.org/10.1002/eqe.4290040306>
- [7] J. Wulff, J.F. Taylor, A.J. Shaler, *Metallurgy for engineers*. John Wiley and Sons, New York, 1956.
- [8] C.E. Birchenall, *Physical metallurgy*. McGraw Hill, London, 1959.
- [9] F. Sadek, B. Mohraz, A.W. Taylor, R.M. Chung, Passive energy dissipating devices for seismic applications. *Report NISTIR 5923. Building and Fire Research Laboratory*. National Institute of Standards and Technology. Gaithersburg, Maryland, 1996. <https://doi.org/10.6028/nist.ir.5923>
- [10] G.W. Rodgers, J.G. Chase, J.B. Mander, Repeatability and high-speed validation of supplemental lead-extrusion energy dissipation devices, *Advances in Civil Engineering*, 1–13, 2019. <https://doi.org/10.1155/2019/7935026>
- [11] G.W. Rodgers, J.G. Chase, J.B. Mander, N.C. Leach, C.S. Denmead, L. Cleeve, D. Heaton, High force-to-volume extrusion dampers and shock absorbers for civil infrastructure, *Progress in Mechanics of Structures and Materials*, 415–420. CRC Press, 2007.
- [12] G.W. Rodgers, Next generation structural technologies: Implementing high force-to-volume energy absorber, Ph.D. Dissertation, *University of Canterbury*, Christchurch, New Zealand, 2009.



- [13] C. Soydan, A. Güllü, O. Hepbostancı, E. Yüksel, E. İrtem, Design of a special lead extrusion damper. *15th World Conference of Earthquake Engineering*, Portugal, 2012.
- [14] C. Soydan, A new beam-to-column connection for the precast concrete structures and evaluation of its performance. Ph.D. Dissertation, *Istanbul Technical University*, Istanbul, Türkiye, 2015.
- [15] V. Vishnupriya, G.W. Rodgers, J.B. Mander, J.G. Chase, Precision design modeling of HF2V devices. *Structures*, **14**, 243–250, 2018. <https://doi.org/10.1016/j.istruc.2018.03.007>
- [16] V. Vishnupriya, Modelling force behaviour and contributions of metallic extrusion dampers for seismic energy dissipation, Ph.D. Dissertation, *University of Canterbury*, Christchurch, New Zealand, 2019.
- [17] V. Quaglini, C. Pettoroso, E. Bruschi, Design and experimental assessment of a prestressed lead damper with straight shaft for seismic protection of structures. *Geosciences*, **12**, 182, 2022. <https://doi.org/10.3390/geosciences12050182>
- [18] C. Soydan, E. Yuksel, E. İrtem, The behavior of a steel connection equipped with lead extrusion damper. *Advances in Structural Engineering*, **17(1)**, 25-39, 2014. <https://doi.org/10.1260/1369-4332.17.1.25>
- [19] T. Bacht, J.G. Chase, G. MacRae, G.W. Rodgers, T. Rabczuk, R.P. Dhakal, J. Desombre, HF2V dissipator effects on the performance of a 3 story moment frame. *Journal of Constructional Steel Research*, **67**, 1843-1849, 2011. <https://doi.org/10.1016/j.jcsr.2011.05.007>
- [20] J. Desombre, G.W. Rodgers, G.A. MacRae, T. Rabczuk, R.P. Dhakal, J.G. Chase, Experimentally validated FEA models of HF2V damage free steel connections for use in full structural analyses. *Structural Engineering and Mechanics*, **37(4)**, 385–399, 2011.
- [21] C.C. Patel, Seismic analysis of parallel structures coupled by lead extrusion dampers, *International Journal of Advanced Structural Engineering*, **9**, 177-190, 2017. <https://doi.org/10.1007/s40091-017-0157-x>
- [22] C. Soydan, E. Yuksel, E. İrtem, Seismic performance improvement of single-story precast reinforced concrete industrial buildings in use. *Soil Dynamics and Earthquake Engineering*, **135**, 106167, 2020. <https://doi.org/10.1016/j.soildyn.2020.106167>
- [23] V. Vishnupriya, G.W. Rodgers, J.G. Chase, Nonlinear finite-element modeling of HF2V lead extrusion damping devices: generic design tool. *Journal of Structural Engineering*, **148(1)**, 04021227, 2022. [https://doi.org/10.1061/\(ASCE\)ST.1943-541X.0003170](https://doi.org/10.1061/(ASCE)ST.1943-541X.0003170)
- [24] F. Çalım, A. Güllü, C. Soydan, E. Yüksel, Development and experimental validation of finite element models for a prestressed lead extrusion damper. *Structures*, **50**, 1114-1125, 2023. <http://doi.org/10.1016/j.istruc.2023.02.094>
- [25] SIMULIA Abaqus/CAE (Vers. 2020) [Computer software]. Vélizy-Villacoublay: Dassault Systems.